

We are IntechOpen, the world's leading publisher of Open Access books Built by scientists, for scientists

6,900

Open access books available

186,000

International authors and editors

200M

Downloads

Our authors are among the

154

Countries delivered to

TOP 1%

most cited scientists

12.2%

Contributors from top 500 universities



WEB OF SCIENCE™

Selection of our books indexed in the Book Citation Index
in Web of Science™ Core Collection (BKCI)

Interested in publishing with us?
Contact book.department@intechopen.com

Numbers displayed above are based on latest data collected.
For more information visit www.intechopen.com



Nanomaterials: An Overview of Nanorods Synthesis and Optimization

*Alsultan Abdulkareem Ghassan, Nurul-Asikin Mijan
and Yun Hin Taufiq-Yap*

Abstract

Nanorods are nanostructures that are the object of fundamental and applied research. They may be prepared from carbon, gold, zinc oxide, and many other materials. They are bigger than individual atoms (measured in angstroms, $1 \text{ \AA} = 10^{-10} \text{ m}$) and also than small molecules. The turning point for nanomaterials research was the discovery of carbon nanotubes in 1991. Their mechanical, electrical, and optical properties depend upon their size, allowing for multiple applications. Also, nanorods may be functionalized for different applications. In this Chapter, the methods of synthesis and analysis, and the applications of carbon, zinc oxide, gold, and magnetic nanorods are reviewed.

Keywords: nanorods, gold nanorods, ZnO nanorods, carbon nanorods, magnetic nanorods

1. Introduction

Nanomaterials are foundations of nanoscience and nanotechnology. The development of nanomaterial has been attracted great interest in the worldwide in the past few years. The turning point for nanomaterials research was the discovery of carbon nanotubes in 1991 [1]. Nanomaterials are usually defined as having a particle size between 1 and 100 nanometers (nm). They are bigger than individual atoms (measured in angstroms, $1 \text{ \AA} = 10^{-10} \text{ m}$). One nanometer is millionth of millimeter. It is equal to 100,000 times smaller than the diameter of human hair. After this discovery, there was an explosive increase in the number of research teams working in the field. The properties of nanomaterials deviate from those of “bulk” materials with the same composition, thus allowing for many interesting applications. At nanodimensions, quantum effects, like quantum confinement, permit multiple applications [2–4]. Some of nanotechnology applications include alternative energy [3], electronics [5, 6], catalysis [5], biomedicine [2], batteries [7], water treatment [8], and materials reinforcement [9] (**Figure 1**).

2. Classification of nanomaterial

Classification is based on the number of dimensions, which are not confined to the nanoscale range ($<100 \text{ nm}$) (**Figure 2** and **Table 1**):



Figure 1. (a) Evolution of science and technology and the future [10]; (b) an example of nanomaterial comparison; and (c) an example of the nanorod image [11].

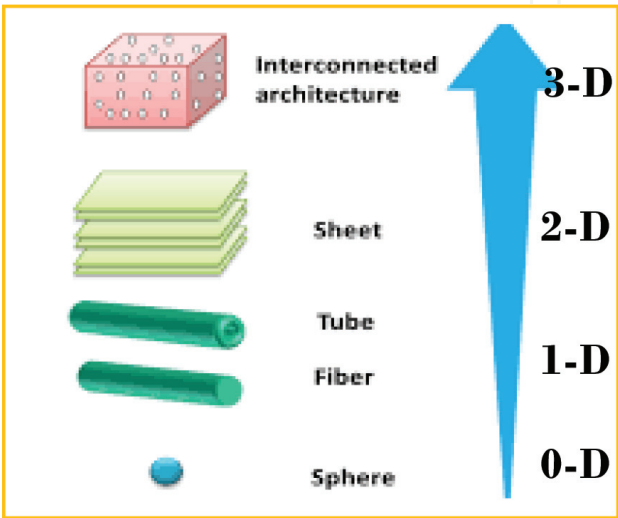


Figure 2. 0-D, 1-D, 2-D and 3-D nanomaterial [12].

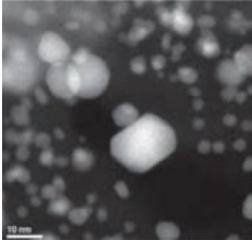
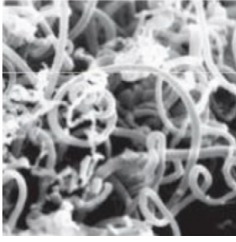
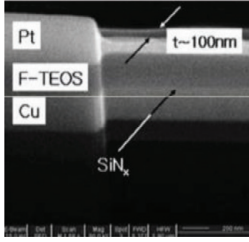
0-D	1-D	2-D	3-D
Material within nanoscale (no dimension or 0-D). It can be amorphous or crystalline (single crystalline or polycrystalline), can be composed of single and multi-element, exhibit various shapes and forms, exist individually or incorporated in matrix, exist in the form of metallic, ceramic or polymeric.	One dimension outside the nanoscale. Exhibit needle like-shaped, the material including nanotubes, nanorods, and nanowires. It can be amorphous or crystalline (single crystalline or polycrystalline), Chemically pure or impure, Standalone materials or embedded in within another medium, exist in the form of metallic, ceramic, or polymeric	Two of the dimension not confine to nanoscale, exhibit plate-like shape, the material including nanofilms, nanolayers and nanocoating. It can be amorphous or crystalline, composed of various chemical composition, deposited on a substrate, exist in the form of metallic, ceramic or polymeric.	Three dimension not confined to the nanoscale, materials possess a nanocrystalline structure, bulk nanomaterials can be composed of a multiple arrangement of nanosize crystals, most typically in different orientations, contain dispersions of nanoparticles, bundles of nanowires, and nanotubes as well as multilayers.
			

Table 1. Details characteristic of nanomaterial classification.

- 1. zero-dimensional (0-D);
- 2. one-dimensional (1-D);
- 3. two-dimensional (2-D); and
- 4. three-dimensional (3-D).

3. One-dimensional (1-D): needle-like shape structure

1-D nanostructures as a series of the most important materials owed by it fascinating physical properties. Due distinct structure-dependent properties had lead it application widely especially in solar energy conversion, thermoelectric devices, energy storage technology. 1-D nanostructures mainly show three different morphologies (**Table 2**):

- i. nanorod;
- ii. nanowires; and
- iii. nanotube.

Among those 1-D nanostructures, nanorods have the advantage as it can be made from most elements (metals and nonmetals) and compounds, and the synthetic requirements for their production are more flexible than for nanotubes and nanowires. Nanorods have typical lengths of 10–120 nm. For example, metallic nanorods, semiconductor nanorods, carbon nanorods, and oxides nanorods, are essential for the development of electronic, optical, magnetic, and micromechanical devices [5, 6].

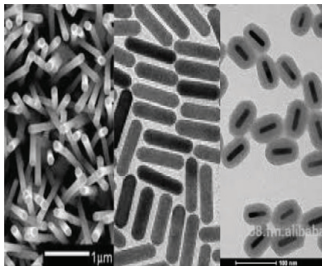
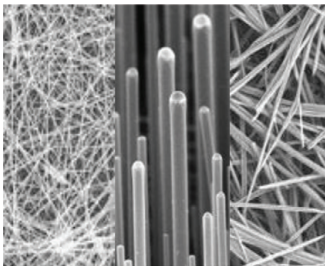
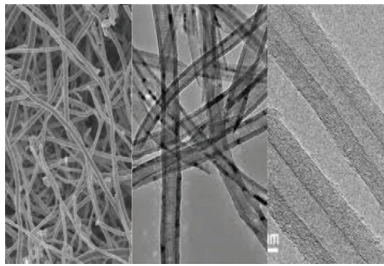
Nanorod	Nanowires	Nanotube [9]
<p>Nanorods similar to nanotube but without internal surface. Less versatile than nanotube but thermally stable Made: carbon, metal oxide, metal Application: drug delivery, bioimaging, photothermal therapy nanocapacitors, etc. [5, 6]</p>	<p>Nanowires have typically diameters of a few tens of nm, but the lengths are not bounded. Made: ceramic, metal oxide, metal Application: magnetic devices, nanowires battery, nanogenerator, semiconductor, etc.</p>	<p>Nanotubes are also like nanowires, in terms of diameter, but hollow and with a standard aspect ratio (length divided by width) of 3–5. Exist as single- or multi-walled. Made: carbon; single-walled carbon nanotubes (SWCNT), multi-walled carbon nanotube (MWCNT) Application: scaffolds or templates for the building [13].</p>
		

Table 2.
Nanorods, nanowires and nanotube.

4. Advantages of nanorods

Due to their shape anisotropy (physical properties), nanorods are attractive component to be studied and ideal candidates for many application. It was discovered that ability of the nanorods was enhanced as compared spherical particles. This is due to the increase of aspect ratio of the particle lead to the increased of excitation of surface plasmons in the nanoparticles. Particularly, the strength of the dipole moment is within a nanoparticle due to incrementing of surface plasmons. Therefore, an increase of surface plasmons lead to the enhancement of electrical field in nanorods as compared spherical particles. One example of benefit of a rod-like shape demonstrated by Alivisatos and co-workers [14] who observed partially aligned CdSe nanorods provided an effective, directed path for charge carriers to move throughout the photovoltaic device and be collected. Similarly, the incorporation of nanorods within P3HT film could improve the external quantum efficiency by a factor of 3 as the aspect ratio increased from 1 to 10. The accumulation of electrons was improved as the aspect ratio of nanoparticles increased. Furthermore, alignment of nanorods also plays a key role in improving it properties. Work by Winey group [15] studying Ag nanorods for polystyrene composites and discovered that the aspect ratio of anisotropic nanoparticle play role in the electrical conductivity of polymer composites. Particularly, due to the minimal percolation threshold of rod-shape particles as compared to spherical particles. Percolation has been found to be depended on both size and shape of nanoparticles. Larger in both length and diameter of rod-shape particles are expected to share many advantages in the oriental properties of nanorods. Last but not least, nanorods offer more advantages over isotropic (homogeneous and uniform) particles. It can be summarized that the efficiency of nanorods depends strongly on nanorods aspect ratio, volume fraction, polydispersity and orientation.

4.1 Type of nanorods and advanced synthesis method

Various nanorods have been extensively studied such as carbon nanorods, ZnO nanorods, gold nanorods and magnetic nanorods. Recently, various techniques have been proposed for synthesizing the nanorods. It can be classified into either via physical or chemical methods or known as bottom-up or top-down techniques. The method such as thermal hydrolysis, hydrothermal route, sol-gel, vapor condensation, spray pyrolysis, pulse laser decomposition, laser ablation, thermal evaporation, pulse combustion-spray pyrolysis, electro-mechanical, flame spray plasma, microwave plasma, low energy beam deposition, ball-milling, chemical vapor deposition, laser ablation, chemical reduction, co-precipitation, hybrid wet chemical route, physical evaporation, electrophoretic deposition, radio frequency (RF) magnetron sputtering, vapor deposition, metal assisted growth, template assisted routes, metal-assisted growth and seed-based growth, simple chemical etching, etc. Typically, nanorods prepared by controlling the nucleation growth than transverse one.

4.1.1 Carbon nanorods

Carbon nanorods have attracted great interest from past few decades owing to their physical (particle size, shape, large surface area and greater pore size distribution) and chemical properties [16–18]. Nanorods made of carbon also known as “carbon nanorods” and “diamond nanorods.” Diamond nanorods have a crystalline structure like diamond with sp^3 carbon hybridization. The yield and purity of

synthesizing the carbon nanorods are strongly dependent on the composition of the inert atmosphere and its pressure. Generally, the carbon nanorods had better physicochemical properties after introducing different functionalities in the carbon nanorods pore surfaces. It will permit many applications, like in catalysis, water treatment, supercapacitors, and others. Carbon nanorods large applied as anodic material in batteries apart from their application like fillers [19] and high performance electrode materials in batteries [20–23]. Till now, various synthesis methods have been proposed and it can be classified as “bottom up” (like synthesis from small molecules or colloidal solutions) or “top down” (like starting with bigger structures). The top-down method for synthesizing carbon nanorods including, simple chemical etching and electrochemical etching. Meanwhile, bottom-up approach including template assisted, metal assisted, hydrothermal route, vapor deposition (CVD), seed based and other synthesis in solution.

A recent finding was discussed on the recent advanced efforts in the preparation of carbon nanorods from metal-organic frameworks (MOFs) [24]. MOFs-a class of porous and crystalline material have attracted a great deal attention due to their fascinating architectures as well as their useful properties [25]. MOFs could be synthesized using both organic and inorganic components. Eventhough MOFs is well-established excellent porous material, yet the thermal transformation of MOFs into carbon materials accompanied by partial or complete collapse of their original morphology. Due to this reasons, the synthesis of nonhollow (solid) 1-D of carbon nanorods with moderate aspect ratio, high surface area and good performance capacitor electrodes is achieved by self-scarified and morphology-preserved thermal transformation of MOF-74 [24] (**Figure 3**).

The reaction of zinc nitrate and 2,5-dihydroxyterephthalic acid in N, N-dimethylformaide (DMF) by traditional hydrothermal method resulted in formation of microcrystalline MOF-74. The room-temperature reaction of those components in the presence of salicylic acid as a modulator led to the formation of rod-shaped MOF-74 (MOF-74-Rod, 30–60 nm wide, 200–500 long) as observed by scanning electron microscopy (SEM) and transmission electron microscopy (TEM).

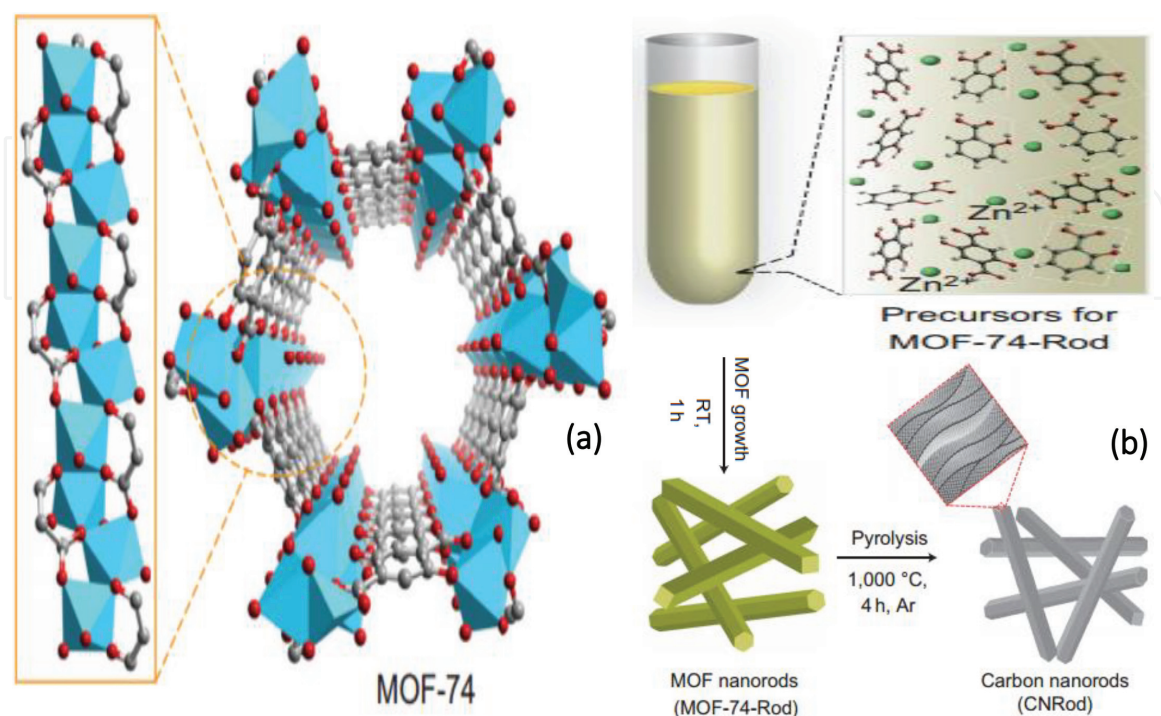


Figure 3.
 (a) The secondary building unit and 3-D crystal structure of MOF-74 and (b) scheme of synthesis of MOF-74-rod, carbon nanorods. (b) The secondary building unit and 3-D crystal structure of MOF-74.

The addition of salicylic acid directed MOF growth in a rod-shape morphology by stabilizing the active metal sites on the MOF crystal surface [26]. The thermal transformation of MOF-74-Rod at 1000°C results in the formation of carbon nanorods. In comparison of MOF-74-Rod ($377 \text{ m}^2 \text{ g}^{-1}$), higher surface area of MOF-74 ($411 \text{ m}^2 \text{ g}^{-1}$) might be attributed to the perfect arrangement of MOF crystallites in the domain structure. The pore size distribution for MOF-74-Rod confirms the formation of micro ($\sim 1.5 \text{ nm}$) and mesopores ($\sim 6.5 \text{ nm}$), whereas MOF-74 shows the presence of micropores ($\sim 1.2 \text{ nm}$) exclusively. The great different in pore size distribution attributed to the formation of voids resulted from lateral attachment of MOF nanorods. The MOF-74-Rod showed excellent capacitor performance with specific capacitance value of 164 F g^{-1} at sweep rate of 10 mVs^{-1} . Overall from this study, open up new avenues for efficient product of 1-D carbon material with promising applications in electrochemical devices.

4.1.2 ZnO nanorods

ZnO has a wide band-gap (3.37 eV at room temperature). ZnO is known to have wurtzite structure with lattice constant (a) 3.249 \AA , (c) 5.207 \AA . It has a large excitonic binding energy of 60 MeV, which is greater than the thermal energy at room temperature, makes it a promising candidate for applications in blue-UV light emission and room-temperature UV lasing. ZnO posed an excellent chemical and thermal stability and the electrical properties. Since ZnO has lack of center symmetry, make it results in a piezoelectric effect, whereby a mechanical stress/strain could be transformed into electrical voltage and vice versa, due to the relative displacement of the cations and anions in the crystal [27]. Single crystal of ZnO exhibit significantly faster electron transport and greater mobility. The faster electron transport is a result of the high electron diffusion coefficients, which will provide significant advantages to device performance [28]. Since ZnO could emits at the near ultraviolet, has transparent conductivity and piezoelectric properties, thus, ZnO is an interesting material for semiconductor and laser devices, piezoelectric transducers, transparent electronics, surface acoustic wave devices, spin functional devices, and gas sensing. Overall, ZnO is an excellent material for sensor application attributed by its large surface to volume ratio that leads to the enhancement of its sensitivity, bio-safety and bio-compatibility. A recent research has demonstrated that creation of highly oriented and ordered array of ZnO nanostructures has greatly stimulate interest in development of novel devices [29]. The large surface area of nanorods makes ZnO attractive for gas and chemical sensing. High oriented array of ZnO nanorods (and nanowires) can be produced via various chemical, electrochemical and physical deposition techniques such as chemical vapor deposition (CVD) or metal organic CVD (MOCVD), vapor-liquid-solid (VLS) growth, electrochemical deposition (ED) and hydrothermal approaches.

Recently, a great deal of attention has been focused on the study of synthesizing the ZnO nanorods via VLS method. In this case, gold (Au) nanoparticles are used as catalyst in order to promoting the ZnO nanorods formation. Unfortunately, there are some apparent drawbacks in VLS growth technique. Generally, it required high growth temperature $> 900^\circ\text{C}$ in order to dissolving the Zn vapor into the Au catalyst simultaneously forming an alloy droplet. After saturated, Zn precipitates out from the droplet and further oxidized as ZnO nanorods grow. The other drawback from VLS growth method is that at the tips of ZnO nanorods there are always impurity particles that might be undesirable for fabrication. Due to this reason, the synthesizing ZnO nanorods via CVD and MOCVD were highlighted. The synthesis temperature used generally mild reaction temperature and high purity of ZnO nanorods could be formed.

Apparently, the CVD process took place in a horizontal quartz tube placed in a rapid thermal furnace. **Figure 4(a)** shows a schematic illustration of the CVD furnace including a horizontal quartz tube of 1-in. A high-purity metallic granulated zinc (99.99%) was placed in an alumina boat which was then inserted at the end of quartz ampoule sealed at one end. Au nanoparticles are used as catalyst deposited on Chip B and C. Once the temperature went above the melting point of zinc metal (420°C), zinc would gradually vaporize to fill the quartz vial and then diffuse to Chip B and then to Chip C. The Au catalyst further formed liquid droplet and super saturated with Zn vapor. The nucleation growth of ZnO started with the arrival of oxygen gas. The ZnO will precipitate when the droplet reached a critical radius and continuously growth. Typically, ZnO synthesis was synthesized follow several steps. Initially, the quartz tube evacuated to 10–2 Torr, follow by purged using Ar gas to maintain a 1 atm ambient. The furnace temperature rapidly increased to 700°C under constant Ar flow and maintain within a period of time. Finally, the oxygen gas (O_2 mixed Ar) was then flown through quartz tube forcing a precipitate to form. As shown in **Figure 4(c)**, shows prismatic hexagonal rods of ZnO grown area. The ZnO crystal continuously growth perpendicular from the surface on one single nanowires forming comb

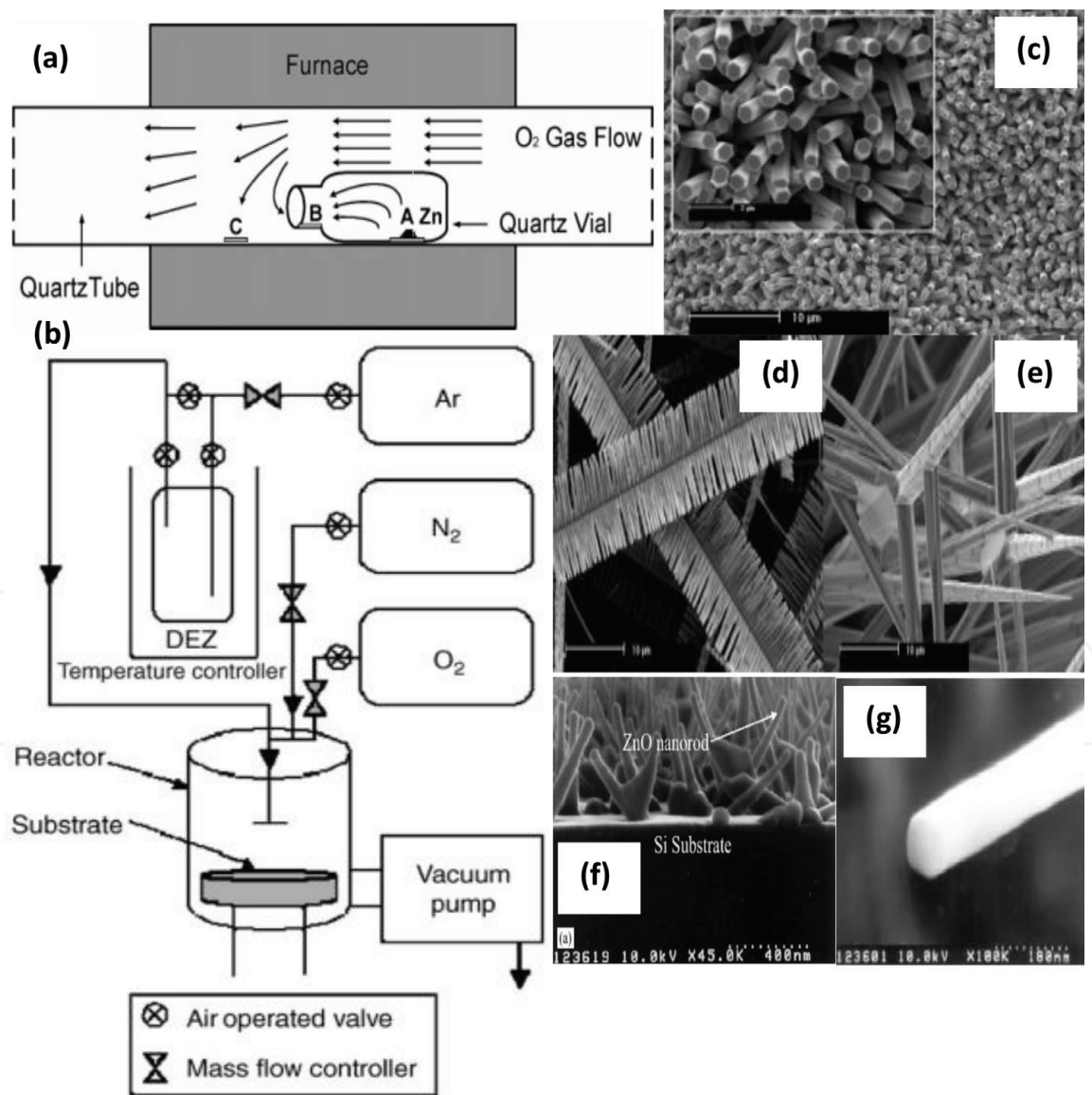


Figure 4. Schematic illustration of the (a) CVD system with a horizontal quartz tube placed in a furnace. A small quartz vial inside the quartz tube is used to trap zinc vapor during the synthesis process, (b) MOCVD system, (c) SEM image for ZnO nanorods from CVD system, (f) SEM image for ZnO nanorods from MOCVD system and (g) SEM image of a ZnO nanorod, indicating a diameter of 110 nm.

structure (**Figure 4(d)**). Thick ZnO needle can be found at the outer edge (**Figure 4(e)**). With sufficient oxygen concentration, wires with larger diameter are grown.

In the case of MOCVD techniques, in MOCVD generally, the use of organic precursor, such as $\text{Zn}(\text{C}_2\text{H}_5)_2$ and O_2 system, are involved. The ZnO films or nanorods were deposited on p-type silicon with (100) orientation. **Figure 4(b)** shows a schematic diagram of the MOCVD system. Mass flow controllers separately controlled the flow of Ar and O_2 gases and the gas flow ratio of Ar to O_2 was in the range of 1–2. The substrate temperature was varied as a process variable ranging from 250 to 500°C [30]. The deposition time was set to 10 min [30]. In this study the SEM image reveals that ZnO nanorods are directly grown on Si substrates (**Figure 4(f)**) and the diameter of ZnO nanorod ranges from 40 to 120 nm (**Figure 4(g)**). In summary, the uniform ZnO nanorods have successfully synthesized in bulk quantities directly on the Si substrate using the MOCVD technique.

Recently, several studies have demonstrates the growth of ZnO nanorods could be achieved molecular beam epitaxy (MBE). In MBE, the growth is performed under clean, low pressure condition and the reactants are very pure Zn metal and atomic O from a plasma generator [31]. In MBE system, the potential contamination is minimized [31]. The ZnO layers typically were grown on p-type silicon wafer Si (100) under conditions: substrate temperature 300–430°C, temperature of the Zn-Knudsen cell 300°C (Zn beads of purity 99.9999 were filled), pressure of the chamber during the growth was $\sim(1-4) \times 10^{-4}$ mbar and oxygen plasma was generated [32]. The ZnO nanorods of reasonable quality could be deposited forming cored nanorod (**Figure 5(a and b)**). This cored nanorods could be produced using Mg-doping during MBE growth. Similarly, Heo et al. [33] report on catalyst-driven MBE of ZnO nanorods. The single ZnO nanorod growth is realized via nucleation on Ag films that are deposited on SiO_2 -terminated Si substrate surface (**Figure 5(c)**). Growth occurs at substrate temperatures within range of 300–500°C. The nanorods are uniform cylinders exhibiting diameter of 15–40 nm (**Figure 5(d)**) and lengths in excess of 1 μm . Eventhough CVD, MOCVD and MBE

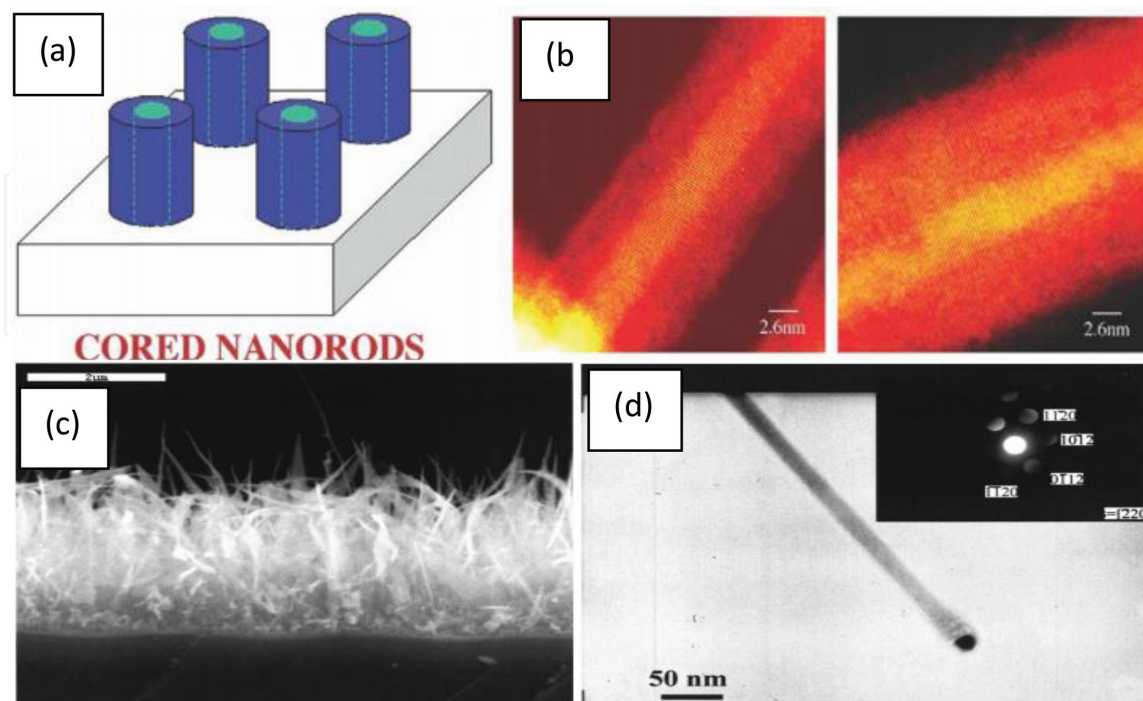


Figure 5. (a) Schematic of coaxial nanorods having a lateral heterostructure (top), (b) transmission electron micrographs showing cored $(\text{Zn}_{1-x}\text{Mg}_x)\text{O}$ nanorods a having Zn-rich phase surrounded by another $(\text{Zn}_{1-x}\text{Mg}_x)\text{O}$ phase (bottom), (c) SEM image of ZnO nanorods nucleated on Ag-coated Si/ SiO_2 substrate and (d) TEM and selected area diffraction image of a single crystal ZnO nanorod.

such an attractive technique in developing ZnO nanorods but these growth techniques are complicated and growth temperatures used are high (435°C).

The hydrothermal method [34, 35] has attracted considerable attention due to its unique advantages-it is simple, low temperature (60–100°C), high yield, low cost, uncomplicated process, excellent morphology-well-defined structure and controllable process [36]. Particularly, chemical precursor solution involves in formation of ZnO nanorods via hydrothermal route is Zn salt and hexamethylenetetramine on Si substrates with a seed layer prepared from zinc acetate solution. Polyethyleneimine was added to the solution to increase the nanorod aspect ratio [37]. The growth temperature and the growth time were constantly kept at lower temperature < 100°C and under certain period of time. Recently, ZnO nanorods with hexagonal structure were synthesized via hydrothermal route by Polsongkram and co-workers using zinc nitrate [$\text{Zn}(\text{NO}_3)_2 \cdot 6\text{H}_2\text{O}$] that was mixed with hexamethylenetetramine (HMT) ($\text{C}_6\text{H}_{12}\text{N}_4$) solution and treated under temperature 60–95°C. It is evident that at 95°C, the sample mainly consists of ZnO nanorods and most of them assembly into branched and urchin-like morphologies (**Figure 6(a)**). It was discovered that the hexagonal ZnO nanorods formed about 2 mm in length 100–150 nm in diameter. The nanorods grown larger (thick branched rods) when the temperature reduce to 75 and 60°C [35] (**Figure 6(c and d)**). This study also found that controlled growth of nanorods ranging from a thinner to a larger diameter can be realized by appropriate choice of the initial precursor concentration and deposition time. The hexagonal ZnO nanorods formation via hydrothermal method also in agreement with Phromyothin findings (**Figure 6(d and e)**) [38]. Similarly, this study also discovered that as the precursor concentration increased, the average diameter of ZnO nanorods will enlarge. It can be suggested that the precursor concentration provides the crucial role on the physical morphology and crystal growth direction of ZnO nanorods.

Last but not least, the ZnO nanorods also could be synthesized via ED method. ED method has many advantages including a low growth temperature, simple and low cost process without the need for vacuum systems for preparing ZnO nanorods with high crystallinity, being suited for scale-up and good electrical contact between the structures and the substrate [39]. However, in ED method when the ZnO nanorods were growth using electrochemical on transparent conducting oxides (TCOs, i.e. ITO and FTO), electrodes and a previously deposited ZnO seed layer are necessary to precisely control the morphology and aspect ratio of the as-grown ZnO nanostructures. In ED method the ZnO nanorods were electrodeposited from the zinc nitride aqueous solution in an electrode system. Typically, electrodepositions were conducted in a water bath at 80°C. **Figure 6(f)** presents the electrodeposited ZnO results, the result showed the SEM images of ZnO nanorods on predeposited PAN film [40]. The ZnO nanorods exhibited good vertical alignment, and with significant hexagonal cross section and a relatively uniform size with an average diameter of 180 nm.

4.1.3 Gold nanorods

Much attention has been given recently to gold nanorods (Au nanorods), mainly due to their applications in biomedicine. Gold nanorods show two absorption bands, known as surface plasmon resonance (SPR) bands, called the TSPR (transverse) in the visible and LSPR (longitudinal) in the near infrared (NIR) region [41]. This last one is useful for medical applications because NIR radiation is the one that penetrates the most in living tissues. The absorbed radiation is converted into heat, thus showing promise for cancer treatment. Also, these nanorods have localized surface plasmon resonances (LSPRs) that allow for unique scientific and technical applications [42]. In particular, the synthesis of well-defined size and shapes

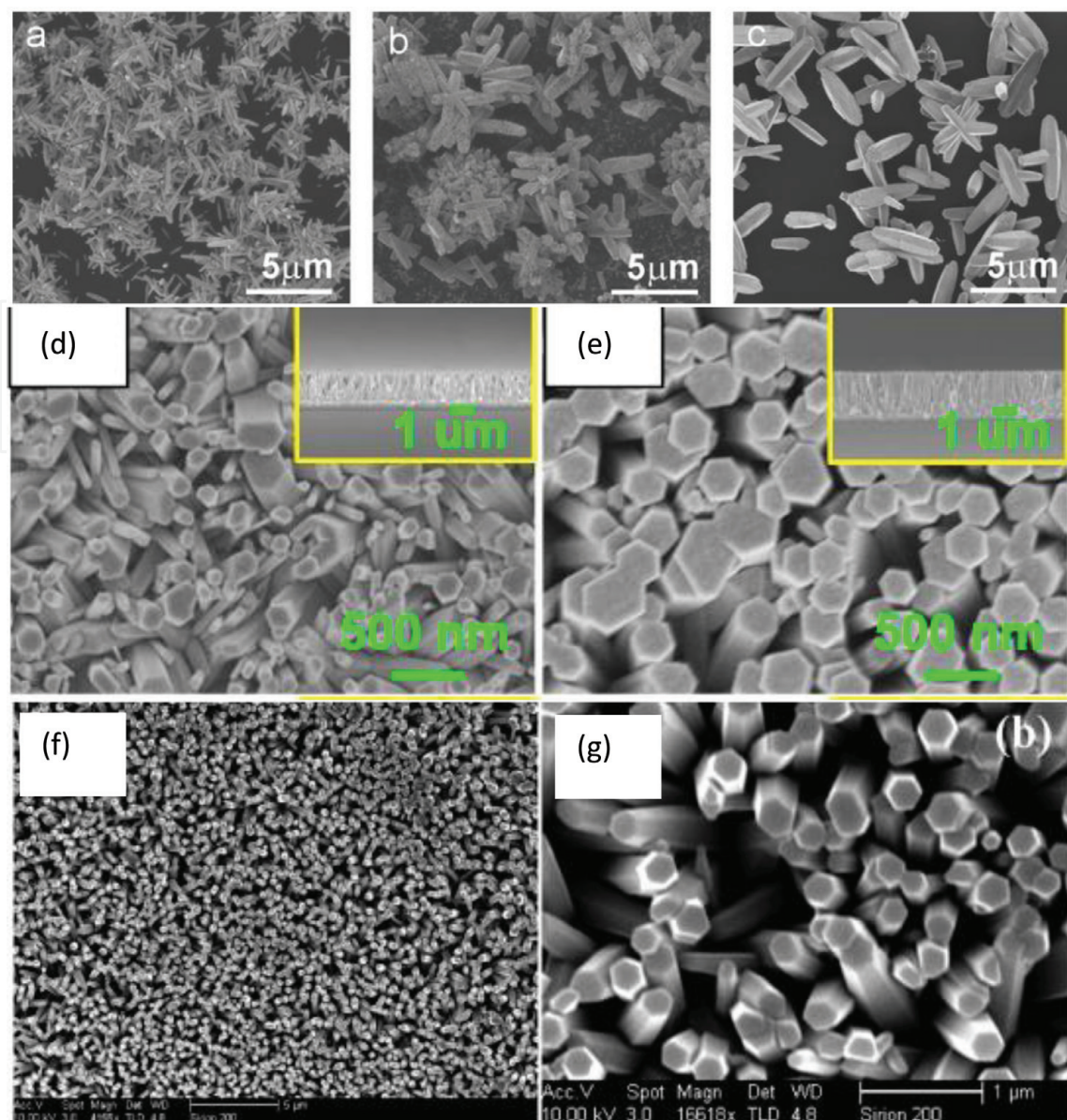


Figure 6.

Scanning electron microscopy (SEM) images of the ZnO nanorods grown from ZnNO_3 -0.040 M: HMT-0.025 M aqueous solution in 30 min at different temperatures: (a) 95°C, (b) 75°C and (c) 60°C [35], (d and e) FESEM images of ZnO nanorods synthesized via hydrothermal method [38] and (f and g) SEM images of ZnO nanorods via ED method.

of Au nanorods has attracted much attention due to its importance in electronic and optical properties of these nanomaterials. The longitudinal bands of Au nanorods can be tuned by changing their aspect ratio, simultaneously make it possible to gain absorption bands at the desired wavelength in the NIR. Small change in aspect ratio will result in drastic change in the NIR absorption wavelength. The Au nanorods could be synthesized via two general growth approaches, which are bottom-up and top-down methods. For bottom-up methods, Au nanorods are generated through nucleation in aqueous solutions and subsequent overgrowth, where Au salts are usually used to provide the Au source through reduction. Particularly, bottom-up method including wet-chemical, electrochemical, sonochemical, solvothermal, microwave-assisted and photochemical reduction technique. All of these method involving the use of reduced aqueous solvated Au salts by various reducing agents, such as sodium borohydride, ascorbic acid, and small Au clusters, under different external stimuli (triggering the reduction of Au salt). The length of Au nanorods could be elongated with the use of template, it serves to confine the growth along one direction during the reduction.

The electrochemical method was the first technique for developing the Au nanorods. Briefly, the Au and Pt were used as the anode and cathode, respectively. These electrodes will be immersed in an electrolytic solution containing the cationic surfactant such as hexadecyltrimethylammonium bromide (CTAB) and co-surfactant. The CTAB works as supporting electrolyte and stabilizer (preventing aggregation of the nanorods), and CTAB induces the formation of rods. The length of the nanorods is determined by the presence of a silver plate in the solution. The silver metals react with the Au ions generated by the dissolution of the anode. The researchers found that the amount of dissolved silver and the concentration of Ag^+ ions determined the length of the nanorods [25]. The larger the area of silver plate, the higher the amount of Ag^+ ion species formed and the higher the speed of silver will be released and thus, the longer the Au nanorods formed [43].

Based on previous literature for Au nanorods formation via bottom-up method, seed mediated growth has been by far the most efficient and popular approach [44]. This method utilizes “soft templates” for growing Au (**Figure 7**), which was developed by Murphy and El-Sayed studies [42]. Highly yield monodisperse Au nanorods with greater uniformity could be developed via this method. Typically, small Au nanoparticles seed of ~ 1.5 nm is initially prepared by reducing chloroauric acid with borohydride in an aqueous CTAB solution [42]. The seed solution will be mixed with growth solution containing metal salt (weak reducing agent) such as ascorbic acid and a surfactant-directing agent CTAB. The CTAB will be absorbed onto Au nanorods forming a bilayer. It is suggested that aspect ratio of Au nanorods can be controlled by ratio metal seed/metal salt in growth solution. According to former study, the CTAB will bind to the crystallographic faces of Au existing along the sides of pentahedrally twinned rods, as compared to the faces at the tip. The seed-mediated growth technique in the presence of CTAB is one of the most widely used and the yields of the nanorods from the seed-mediated growth method can be as high as 99%. It has been reported that the size and shape of Au

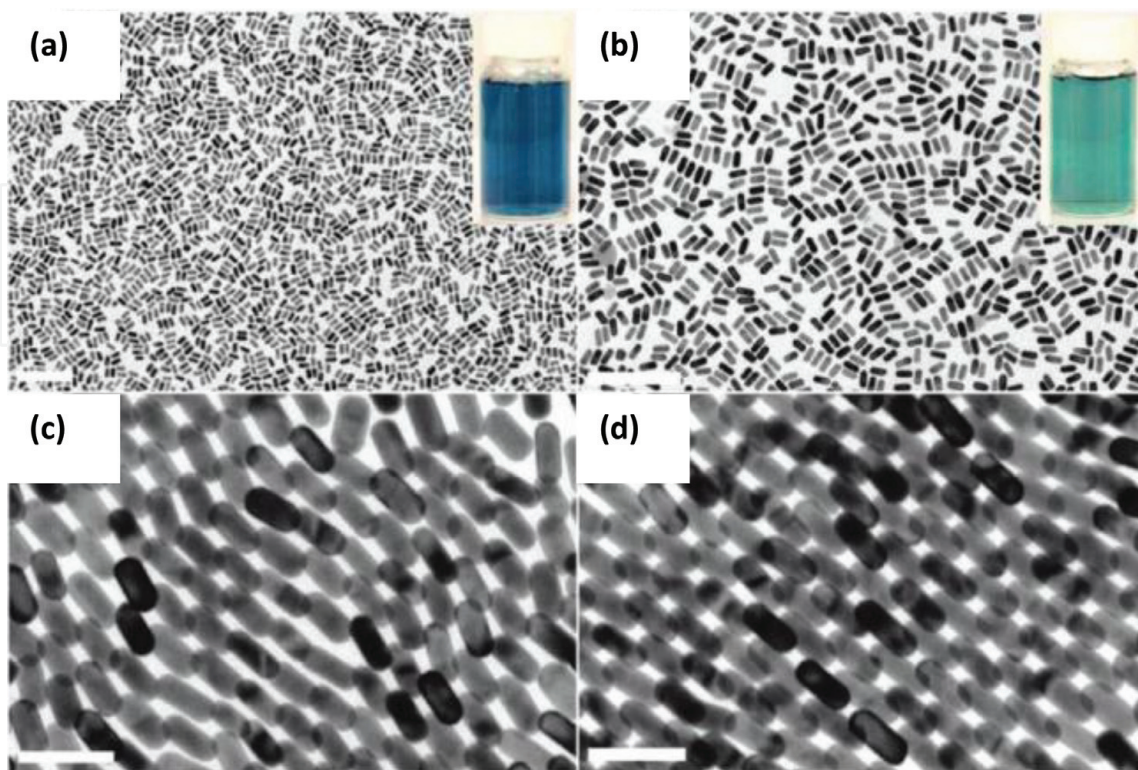


Figure 7.
 (a–d) TEM images for Au nanorods synthesized via seed-mediated growth with the addition of aromatic additive [45].

nanorods could be tailored by adjusting the growth condition such as the pH of growth solution, composition of surfactant, amount of the reagent, growth temperature and structure of the seed in the seed-mediated growth process. Interestingly, recent study demonstrated high yield and greater uniformity of Au nanorods could be obtained via seed-mediated growth through the use of aromatic additive to CTAB [45]. **Figure 7(a and c)** showed TEM images of Au nanorods synthesized with 0.0126 M sodium 3-methylsalicylate (additive) present in the growth solution. The nanorods obtained have an average diameter of 14.0 (1.0 nm and a length of 33.0 ± 2.5 nm. On the other hand, slightly longer nanorods are made when 0.010 M sodium salicylate is used as the additive (**Figure 7(b and d)**).

Eventhough the bottom-up method results in excellent monodisperse Au nanorods with small diameter and high uniformity, yet them suffer some drawback where typically, selective placement of Au nanorods at desired locations on substrates by the bottom-up methods has been very difficult owing to the random nature of the reduction of Au ions and the deposition of Au atoms in reaction solutions. Moreover, the shape and size of Au nanorods also varied from different synthesis batches. This will affect their optical and catalytic properties and applications. Last but not least, bottom-up method suffers in placing Au nanorods into large-area, ordered arrays. Due to these reasons, top-down approaches gained interest.

It is well-established that top-down method could promote high production homogeneous Au nanorods with controlled particle geometries and regular inter-particle arrangements, which is valuable for quantitative characterization as well as device applications. In top-down methods, Au nanorods are obtained through a combination of different physical lithography processes and Au deposition [42]. Particularly, there are two technique used for top-down method in synthesizing the Au nanorods. First method is through the removal of Au from predeposited Au films using ion beam or etching techniques. Second method is by employing the lithography techniques to create mask. Au layer then deposited on the substrate which is covered by the mask via physical method: thermal, electron-beam evaporation or sputtering. The synthesized Au nanorods further obtained from lift-off process. Generally, the size of Au nanorods obtained via top-down method is limited by the resolution of lithography method. Interestingly, recent study by Koh and co-worker reported that state-of-the-art electron beam lithography system able to produce the size of Au nanorods within diameter ranging from ~ 10 to >100 nm [46]. The Au nanorods were fabricated on 30-nm-thick silicon-nitride (SiN) membranes (**Figure 8(a)**). High-resolution TEM images of individual nanostructures of Au nanorods in **Figure 8(b)** reveal that the Au nanostructures

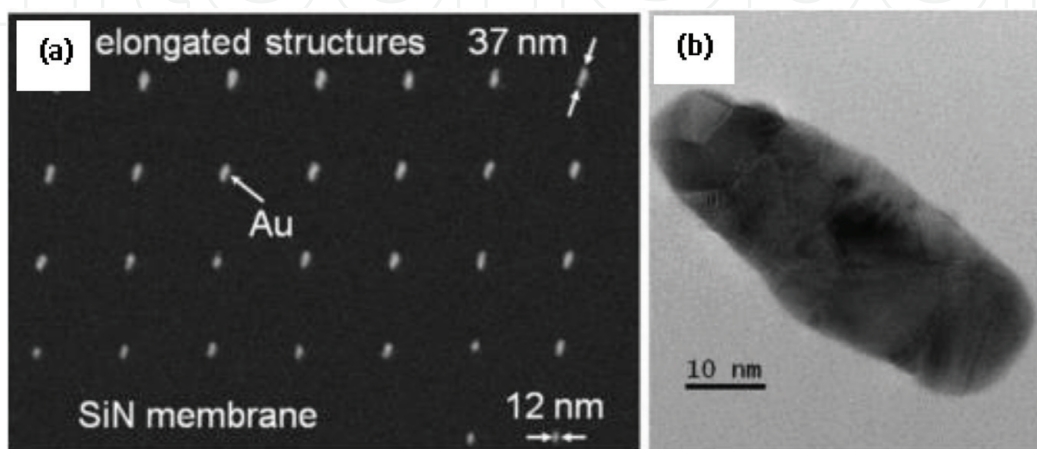


Figure 8.

(a) SEM images of an array of Au nanostructures with elongated and (b) TEM image of individual Au nanorods [46].

were polycrystalline in nature. The polycrystallinity of the metal structures could potentially be a drawback of lithographically defined metal structures, as chemically synthesized metal nanoparticles can be a single crystal when synthesized in certain conditions. Eventhough, Au nanorods successfully synthesized via top-down method yet this method is time consuming and costly makes them impractical for fabrication of Au nanorods in bigger scales. Furthermore, Au nanorods obtained from vacuum deposition techniques also can degrade their plasmonic properties due to the electron scattering at the grain boundaries. Due to these reason had limit their usage in device application and simultaneously make the top-down method to be unattractive in fundamental research.

4.1.4 Magnetic nanorods

Nanostructured iron oxide magnetite (Fe_3O_4) behaves supermagnetic and widely used in the biomedical field as well as device application. Generally, the magnetic nanoparticle could be utilized as nanoadsorbents, cancer diagnostic and treatment, contrast agent in magnetic resonance imaging (MRI), etc. Meanwhile for 1-D magnetite extremely important in building block for nanodevices. It has been found that size and shape of magnetite nanoparticles play key role in controlling the corresponding properties [47]. The magnetite nanoparticles could be synthesis via aqueous co-precipitation, magnetic field induction, CVD, template mediated, etc. [48–50]. The aqueous co-precipitation of Fe^{2+} and Fe^{3+} by a base, usually sodium hydroxide or aqueous ammonia, is the well-known method which is usually carried out for synthesizing the magnetite nanoparticle [51]. This method is the most scalable chemical synthesis routes which results in iron oxide nanospherical crystal. However, there is a study also found that innovative modification in co-precipitation technique through incorporation of special aqueous solution will lead to the formation of nanocubes or nanorods iron oxide particle's. This was in agreement with Khalil finding's [52].

Recently, considerable attention has been drawn to production of 1-D magnetite nanorods due to their high surface to volume ration and superior properties. Due to the high aspect ratio, magnetic nanorods have the high values of coercivity and produce a lot of heat in high frequency magnetic field, which offer longer blood circulation times, stronger interaction with tumors, enhanced retention at tumor sites and improved targeting efficiency [47, 53]. All of these reasons stimulate their making in excellent candidates as targeting pharmaceutical carrier or MRI contrast agents. For instance, iron oxide nanocubes including nanorods structure with a length larger than 100 nm could be achieved via thermal decomposition, wet chemical, hydrothermal, template mediated, solvothermal, hydrolysis and sol-gel.

Thermal decomposition method involved chemical decomposition at high temperature, lead to the breaking of the chemical bonds. The thermal decomposition method for synthesis iron oxide nanorods involve metal-organic compound. The obtained nanorods generally with diameter and length within range of 50–100 nm. This method typically led large nanorods structure due to the annealing by high reaction temperature. It is in agreement with Chen et al. finding reported that with the increasing reaction temperature, the aspect ratio of the products decreases to some extent, thus no any rod-like particles produced when high temperatures synthesis method is used [54]. Meanwhile, eventhough the co-precipitation method is a conventional method for synthesizing iron oxide nanorods, yet this method often uses trioctylphosphine (TOP), tributylphosphine (TBP), trioctylphosphine oxide (TOPO) or oleylamine (OA) and other long chain amines as solvents and capping agents in order to prevent the uncontrolled precipitation. Since this nanoparticle used for biomedical application, hence the nanoparticles of iron oxides

should be a nontoxic. The usage of nontoxic capping agent and stabilizer eliminates the use of toxic and expensive chemical such as TOP, TBP or amines.

In the past years, the wet chemical synthesis of iron oxide nanorods via one step wet chemical method have been reported by several groups [54, 55]. Chen's group reported in the one-step synthesis method and a surfactant, polyethylene glycol (PEG) was used as template and ferrous ammonia sulfate was use as precursor [54]. This study agreed that a formation of iron oxide nanorods can be achieved at longer retention synthesis time and adjusting the diffusion of ammonia by implementation a suitable ratio between the rates of deposition and oxidation of ferrous ions. These were in agreement with TEM image the iron oxide synthesise at from 2 to 10 h and it is reveals that the iron oxide nanorods could be obtained upon extended reaction time. By adjusting pressure of ammonia, i.e., adjusting the concentration of aqueous ammonia in the right flask also results in formation of pure magnetite phase. Further study on synthesizing iron oxide nanorods via wet chemical method were also reported by Ahmed and co-worker [56]. The obtained nanoparticles were rod shaped and consisted mainly of maghemite ($\gamma\text{-Fe}_2\text{O}_3$) phase. The nanoparticles also appear superparamagnetic behavior under room temperature.

Solvothermal method is an effective method for producing iron oxide nanorods. Si et al. present a method for obtaining the iron oxide nanorods via solvothermal method, and product showed formation of iron oxide nanorods with diameter size within range of 58–250 nm and width from 8 to 64 nm (**Figure 9(a and b)**) [57]. The iron oxide nanorods obtained exhibit uniform size and greater dispersion in

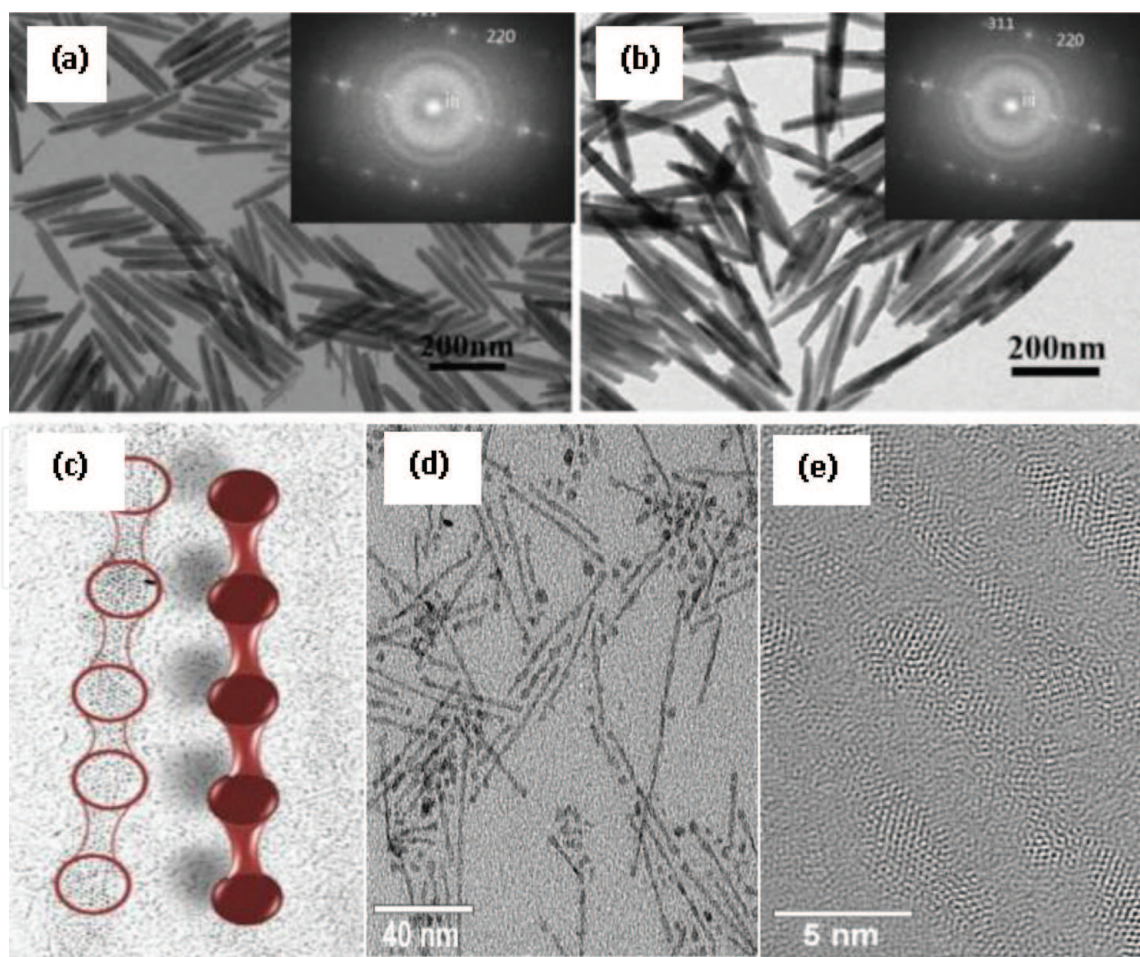


Figure 9. TEM image of iron oxide nanorods in (a) cyclohexane and (b) water prepared via solvothermal method [57], (c) iron oxide nanorods mechanism via template mediated approach, (d) TEM image of the iron oxide nanorods, and (e) high resolution TEM image of iron oxide nanorods synthesized via template mediated approach [59].

nonpolar solvent (cyclohexane). It also revealed the single crystalline nature of nanorods is successfully produced upon synthesis process. The effectiveness of solvothermal method in producing iron oxide nanorods was in agreement Sun and co-worker finding, which reported that Fe_3O_4 single crystal nanorods with a uniform length between 64 and 140 nm can be prepared using $\text{Fe}(\text{CO})_5$ in the presence of oleic acid through a solvothermal process [58].

Recent by Kloust et al. also discovered that the iron oxide nanorods can be produced directly from template mediated approach [59]. The iron oxide nanorods synthesis directly from iron oleate in one-step procedure. The iron oleate is used as a precursor. In this method, the iron oxide nanodot string together in a row to form rods-structure (**Figure 9(c)**). Based on the TEM image the formed iron nanorods exhibit a mean length of approximately 24 nm and mean diameter 2.5 nm with an associated aspect ratio of 10 (**Figure 9(d)**). The iron oxide nanorods produced particularly small and thin nanorods. The nanodot string combination mechanism have been confirmed in TEM micrograph, which shows the alignment of single dot characteristic. The high resolution TEM image of iron oxide nanorods (**Figure 9(e)**) confirms this characteristic and show twisted crystal-orientations of single nanocrystal. Further magnetic characterization reveals that the iron oxide nanorods synthesized via template mediated approach posed super-paramagnetic behavior. In the blocked state the nanorods exhibit a magnetic easy axis parallel to the long axis of nanorods due to the enhancement shape anisotropy. Kloust et al. [59] also presented a method for preparation of iron oxide nanorods with a template approach, where iron oxide nanodots string together. The procedure uses iron oleate as a precursor and is a one-step synthesis. A precise tuning of the width of the nanorods between 1 and 6 nm was realized.

Hydrothermal method might flexible method for synthesizing iron oxide nanorods. Thus, several procedures have been developed [48–50]. Hydrothermal methods rely on the ability of water at elevated pressures and temperatures to hydrolyze and dehydrate metal salts, and the very low solubility of the resulting iron oxide in water at these conditions to generate supersaturation [60]. Extremely high supersaturation could be achieved in the reaction process attributed by the lower solubility of metal hydroxides and oxides, thus very fine crystals will form. Similar case with thermal decomposition methods, the hydrothermal system also involves high temperature synthesis condition. Thus, the size of the nanoparticles had a larger particle (if the hydrothermal method proceed under supercritical temperature ($< 350^\circ\text{C}$)). This was due to the promotion of crystal growth that results from the dissolution and precipitation process in sub-critical water. The particle size also increased with the increase in reaction pressure in supercritical water [61]. Liang and co-workers report the variation of crystallite and particles size of iron oxide at temperature 250 and 350°C ; the crystallite size of iron oxide increased significantly as the temperature was raised from 250 to 350°C . This phenomenon is due to the nucleation process which occurred as the monomer concentration reached the saturation point [62]. Interestingly, the size of particles will reduce and become smaller if the hydrothermal method proceeded under temperature $> 380^\circ\text{C}$ (above critical temperature). This is probably due to a rather low solvent power of supercritical water and an extremely high hydrolysis rate of iron salt in supercritical water. Therefore, very high super-saturation is achieved in which results in fine iron oxide crystals nucleating in situ immediately. It is in agreement with Arai et al. study [61]. Eventhough hydrothermal method considered effective in synthesizing iron oxide nanoparticles, yet the particles shape difficult to control in order to form pure rod-like structure.

Other method that effective in synthesizing the iron oxide nanorods is sol-gel method. Piao et al. reported on wrap-bake-peel process for nanostructural

transformation from β -FeOOH nanorods to biocompatible iron oxide nanocapsules [63]. This process involves silica coating, heat treatment and lastly the removal of silica layer, in order to transform the phases and structures of nanostructured materials while preserving their nanostructural characteristic. Water dispersible hollow iron oxide nanocapsules were obtained by applying the wrap-bake-peel process to β -FeOOH nanoparticles. The synthesized magnetite nanocapsules could be successfully used not only as a drug-delivery vehicle, but also as a T2 MRI contrast agent.

5. Optimization of nanorods material production

Although the process of synthesis of metallic nanoparticles provides a number of benefits, it is still difficult to achieve formation of nanoparticles of various shapes and sizes, which is significant as shape and size dictate possible nanoparticle activity. Therefore, regulation of nanoparticle shape and size has received a great deal of attention. When marine microbes were employed to synthesize metallic nanoparticles, consideration was given to a range of factors related to metallic nanoparticle nucleation and formation. More specifically, to achieve metallic nanoparticles of uniform size and shape, the factors of pH, reaction temperature, time and reactant concentrations were taken into account.

5.1 pH

The development of metallic nanoparticles depends significantly on the pH of the reaction medium [64]. Gold nanoparticles mediated by *Rhodopseudomonas* capsulate occurred at pH ranging between 4 and 7, while extracellular formation of gold nanoparticles of round shape and 10–20 nm in size occurred at pH 7 and a number of nanoplates occurred at a pH value of 4. Comparable results were obtained when *Shewanella* algae were used to synthesize gold nanoparticles intracellularly under conditions without oxygen and with H_2 gas serving as electron donor at a temperature of 25°C [65]. Thus, gold nanoparticles of 10–20 and 15–200 nm in size respectively occurred in periplasmic space with pH 7 and on bacterial surface with pH 2.8. Hence, it can be concluded that pH has great significance for morphological modulation and detection of nanoparticle development site.

5.2 Temperature

The dependence of microorganism-based synthesis of metallic nanoparticles as well as nanoparticle morphology and yield on the temperature of reaction is well established. In a recently conducted study, silver nanoparticles were synthesized extracellularly by *Phoma glomerata* supernatant under conditions of bright sunlight [66]. The maximum yield of silver nanoparticles was achieved at 25°C, while the temperatures of 90, 65, 37 and 4°C were associated with gradually diminishing yield. Furthermore, alkaline pH enabled synthesis optimization. A different study introduced silver nitrate solution in cell-free filtrate of fungus *Trichoderma viride* and silver nanoparticles were synthesized under conditions without light and at different temperatures for a period of 1 day. Thus, round-shaped silver nanoparticles of 2–4 nm in size formed at 40°C, round- and rod-shaped nanoparticles of 10–40 nm in size were observed at 27°C, and nanoplates of 80–100 nm in size formed at 10°C [67].

5.3 Time

Metallic nanoparticle size and shape also depend on the synthesis reaction time. One study employed *Vibrio alginolyticus* supernatant to synthesize silver nanoparticles extracellularly and observed that the greater the reaction time the higher the yield was, while the UV-vis peak was maintained more or less unchanged; on the other hand, the UV-vis peak shifted toward higher wavelength in the context of intracellular synthesis [68]. The conclusion derived was that extracellular synthesis of silver nanoparticles had time-dependent yield but size was unaffected. However, intracellular synthesis was associated with size enlargement as the reaction time was increased. Comparable results were obtained by a different study that undertook extracellular synthesis of silver and gold nanoparticles by employing single-cell protein (*Spirulina platensis*) [69]. Nanoparticles expanded in size as the reaction time was increased, whilst also showing greater aggregation and greater instability [70]. Another study synthesized various metallic nanoparticles with a range of microorganism species and observed that yield increased in direct proportion with reaction time increase [71].

5.4 Concentration of reactants

The development of metallic nanoparticles is subject to the influence of reactant concentration as well. One study reported that the size and shape of gold nanoparticles were considerably impacted by the use of different gold salt concentration alongside *Penicillium brevicompactum* supernatant in reaction medium [72]. Gold salt concentrations of 1 and 2 mM respectively resulted in round gold nanoparticles of 10–50 and 10–70 nm nanoparticles. Furthermore, hexagonal and triangular particles developed when round nanoparticles were added. Nanoparticles of 50–120 nm with particles of different shapes (round, triangular, diamond-like) developed at gold salt concentration of 3 mM. A different study also found that lower and higher metal salt concentrations respectively led to the development of round nanoparticles and triangular and hexagonal nanoplates [73]. Moreover, there is evidentiary support that increase in yeast extract concentration leads to the development of nanoparticles of reduced size [74], while increase in fungal filtrate concentration intensifies development of nanoparticles [66]. In addition, a study highlighted that manipulation of parameters of environment and nutrition enabled synthesizing nanoparticles with control of size and shape [71]. Thus, the above evidence confirms that regulation of metallic nanoparticle size and shape is significantly dependent on reactant concentration.

6. Conclusion

In summary, uniform 1-D magnetite nanorods showed fascinating physical properties this due to the distinct structure-dependent properties of nanorods structures. Larger in both length and diameter of rod-shape particles are expected to share many advantages in the oriental properties of nanorods. Last but not least, nanorods offer more advantages over isotropic (homogeneous and uniform) particles. It can be summarized that the efficiency of nanorods depends strongly on nanorods aspect ratio, volume fraction, polydispersity and orientation. There are many methods for synthesizing carbon nanorods, ZnO nanorods, Au nanorods and iron oxide nanorods. Overall, bottom-up was very effective method for synthesizing nanorods particles. Yet, bottom-up method still suffer with some drawbacks; placing metal into large area, ordered array and purity problem. Due to these

reasons, top-down approaches gained interest, but top-down method is time consuming and costly for industrial practical.

Acknowledgements


The authors acknowledge the financial support from the PUTRA grant-UPM (Vot No: 9344200), MOSTI-e Science (Vot No: 5450746), Geran Putra Berimpak (GPB) UPM/800-3/3/1/GPB/2018/9658700 and University of Malaya's RU grant (Project No:RU007C-2017D).

Author details

Alsultan Abdulkareem Ghassan*, Nurul-Asikin Mijan and Yun Hin Taufiq-Yap
Faculty of Science, Catalysis Science and Technology Research Centre (PutraCat),
Universiti Putra Malaysia, UPM Serdang, Selangor, Malaysia

*Address all correspondence to: kreem.alsultan@yahoo.com

IntechOpen

© 2019 The Author(s). Licensee IntechOpen. This chapter is distributed under the terms of the Creative Commons Attribution License (<http://creativecommons.org/licenses/by/3.0>), which permits unrestricted use, distribution, and reproduction in any medium, provided the original work is properly cited. 

References

- [1] McDonnell T, Korsmeyer S. Helical microtubules of graphitic carbon. *Nature*. 1991;**354**:56-58
- [2] Marangoni VS, Cancino-Bernardi J, Zucolotto V. Synthesis, physico-chemical properties, and biomedical applications of gold nanorods—A review. *Journal of Biomedical Nanotechnology*. 2016;**12**:1136-1158. DOI: 10.1166/jbn.2016.2218
- [3] Kislyuk VV, Dimitriev OP. Nanorods and nanotubes for solar cells. *Journal of Nanoscience and Nanotechnology*. 2008;**8**:131-148. DOI: 10.1166/jnn.2008.N16
- [4] Terrones M, Hsu WK, Kroto HW, Walton DRM. Nanotubes: A revolution in materials science and electronics. *Topics in Current Chemistry*. 1999;**199**: 189-234. DOI: 10.1007/3-540-68117-5_6
- [5] Li Y, Yang XY, Feng Y, Yuan ZY, Su BL. One-dimensional metal oxide nanotubes, nanowires, nanoribbons, and nanorods: Synthesis, characterizations, properties and applications. *Critical Reviews in Solid State and Materials Sciences*. 2012;**37**: 1-74. DOI: 10.1080/10408436.2011.606512
- [6] Patzke GR, Krumeich F, Nesper R. Oxidic nanotubes and nanorods—Anisotropic modules for a future nanotechnology. *Angewandte Chemie International Edition*. 2002;**41**: 2446-2461. DOI: 10.1002/1521-3773(20020715)41:14<2446::AID-ANIE2446>3.0.CO;2-K
- [7] Ruska M, Kiviluoma J. Renewable electricity in Europe: Current state, drivers, and scenarios for. *VTT Tied—Valt Tek Tutkimusk*. 2011;**2020**:1-72. DOI: 10.1039/c1ee01598b
- [8] Chong MN, Jin B, Chow CWK, Saint C. Recent developments in photocatalytic water treatment technology: A review. *Water Research*. 2010;**44**:2997-3027. DOI: 10.1016/j.watres.2010.02.039
- [9] Esawi AMK, Farag MM. Carbon nanotube reinforced composites: Potential and current challenges. *Materials and Design*. 2007;**28**: 2394-2401. DOI: 10.1016/j.matdes.2006.09.022
- [10] Bhat MA, Nayak BK, Nanda A, Lone IH. Nanotechnology, metal nanoparticles, and biomedical applications of nanotechnology. In *Oncology: Breakthroughs in Research and Practice*. IGI Global; 2017. pp. 311-341
- [11] González-Rubio G, Díaz-Núñez P, Rivera A, Prada A, Tardajos G, González-Izquierdo J, et al. Femtosecond laser reshaping yields gold nanorods with ultranarrow surface plasmon resonances. *Science* (80-). 2017;**358**:640-644. DOI: 10.1126/science.aan8478
- [12] Sajanlal PR, Sreeprasad TS, Samal AK, Pradeep T. Anisotropic nanomaterials: Structure, growth, assembly, and functions. *Nano Reviews*. 2011;**2**:5883. DOI: 10.3402/nano.v2i0.5883
- [13] Genck W. Science and technology of the twenty-first century: Synthesis, properties, and applications of carbon nanotubes. *Chemical Engineering Progress*. 2008;**104**:22-24. DOI: 10.1146/annurev.matsci.33.012802.100255
- [14] Mutiso RM, Sherrott MC, Rathmell AR, Wiley BJ, Winey KI. Integrating Simulations and Experiments to Predict Sheet Resistance and Optical Transmittance in Nanowire Films for Transparent Conductors. *ACS nano*; 2013;**7**(9):7654-7663
- [15] Hore MJ, Composto RJ. Functional Polymer Nanocomposites Enhanced by

Nanorods. *Macromolecules*. 2013;**47**(3): 875-887

[16] Rao MV, Amareshwari VV, Mahender C, Himabindu V, Anjaneyulu Y. Flame synthesis of carbon nanorods with/without catalyst. *International Journal of Innovation and Applied Studies*. 2013;**3**:1-5

[17] Abdulkareem-Alsultan G, Asikin-Mijan N, Lee HV, Taufiq-Yap YH. A new route for the synthesis of La-Ca oxide supported on nano activated carbon via vacuum impregnation method for one pot esterification-transesterification reaction. *Chemical Engineering Journal*. 2016;**304**:61-71

[18] Abdulkareem-Alsultan G, Asikin-Mijan N, Lee HVV, Albazzaz AS, Taufiq-Yap YH. Deoxygenation of waste cooking to renewable diesel over walnut shell-derived nanorode activated carbon supported CaO-La₂O₃ catalyst. *Energy Conversion and Management*. 2017;**151**: 311-323. DOI: 10.1016/j.enconman.2017.09.001

[19] Herrera-Ramirez JM, Perez-Bustamante R, Aguilar-Elguezabal A. An overview of the synthesis, characterization, and applications of carbon nanotubes. *Carbon-Based Nanofillers and Their Rubber Nanocomposites*. 2019:47-75. DOI: 10.1016/B978-0-12-813248-7.00002-X

[20] Yuan Z, Dong L, Gao Q, Huang Z, Wang L, Wang G, et al. SnSb alloy nanoparticles embedded in N-doped porous carbon nanofibers as a high-capacity anode material for lithium-ion batteries. *Journal of Alloys and Compounds*. 2019;**777**:775-783. DOI: 10.1016/j.jallcom.2018.10.295

[21] Abdulkreem-Alsultan G, Islam A, Janaun J, Mastuli MSS, Taufiq-Yap Y-H, et al. Synthesis of structured carbon nanorods for efficient hydrogen storage. *Materials Letters*. 2016;**179**:57-60. DOI: 10.1016/j.matlet.2016.05.030

[22] Abdulkareem-Alsultan G, Asikin-Mijan N, Mansir N, Lee HV, Zainal Z, Islam A, et al. Pyro-lytic de-oxygenation of waste cooking oil for green diesel production over Ag₂O₃-La₂O₃/AC nano-catalyst. *Journal of Analytical and Applied Pyrolysis*. 2018;**137**:171-184. DOI: 10.1016/j.jaap.2018.11.023

[23] Alsultan A, Mijan A, Taufiq-Yap YH. Preparation of activated carbon from walnut shell doped La and Ca catalyst for biodiesel production from waste cooking oil. *Materials Science Forum*. Trans Tech Publications; 2016; **840**:348-352

[24] Pachfule P, Shinde D, Majumder M, Xu Q. Fabrication of carbon nanorods and graphene nanoribbons from a metal-organic framework. *Nature Chemistry*. 2016;**8**:718-724. DOI: 10.1038/nchem.2515

[25] Pérez-Juste J, Pastoriza-Santos I, Liz-Marzán LM, Mulvaney P. Gold nanorods: Synthesis, characterization and applications. *Coordination Chemistry Reviews*. 2005;**249**: 1870-1901. DOI: 10.1016/j.ccr.2005.01.030

[26] Yu D, Yazaydin AO, Lane JR, Dietzel PDC, Snurr RQ. A combined experimental and quantum chemical study of CO₂ adsorption in the metal-organic framework CPO-27 with different metals. *Chemical Science*. 2013;**4**:3544-3556. DOI: 10.1039/c3sc51319j

[27] Wahab HA, Salama AA, El-Saeid AA, Nur O, Willander M, Battisha IK. Optical, structural and morphological studies of (ZnO) nano-rod thin films for biosensor applications using sol gel technique. *Results in Physics*. 2013;**3**: 46-51. DOI: 10.1016/j.rinp.2013.01.005

[28] Dharmanto SH, Sebayang D. The simple fabrication of nanorods mass production for the dye-sensitized solar

- cell. In: MATEC Web Conf. 2017. p. 101. DOI: 10.1051/mateconf/201710103006
- [29] Li Q, Kumar V, Li Y, Zhang H, Marks TJ, Chang RPH. Fabrication of ZnO nanorods and nanotubes in aqueous solutions. *Chemistry of Materials*. 2005;**17**:1001-1006. DOI: 10.1021/cm048144q
- [30] Kim KS, Kim HW. Synthesis of ZnO nanorod on bare Si substrate using metal organic chemical vapor deposition. *Physica B: Condensed Matter*. 2003;**328**: 368-371. DOI: 10.1016/S0921-4526(02) 01954-3
- [31] Norton DP, Heo YW, Ivill MP, Ip K, Pearton SJ, Chisholm MF, Steiner T. ZnO: Growth, doping and processing. *Materials today*; 2004;**7**(6):34-40
- [32] Asghar M, Mahmood K, Raja MY, Hasan MA. Synthesis and characterization of ZnO nanorods using molecular beam epitaxy. *Advances in Materials Research*. 2012;**622-623**: 919-924. DOI: 10.4028/www.scientific.net/AMR.622-623.919
- [33] Heo YW, Varadarajan V, Kaufman M, Kim K, Norton DP, Ren F, et al. Site-specific growth of ZnO nanorods using catalysis-driven molecular-beam epitaxy. *Applied Physics Letters*. 2002;**81**:3046-3048. DOI: 10.1063/1.1512829
- [34] Song J, Baek S, Lim S. Effect of hydrothermal reaction conditions on the optical properties of ZnO nanorods. *Physica B: Condensed Matter*. 2008;**403**: 1960-1963. DOI: 10.1016/j.physb.2007. 10.337
- [35] Polsongkram D, Chamninok P, Pukird S, Chow L, Lupan O, Chai G, et al. Effect of synthesis conditions on the growth of ZnO nanorods via hydrothermal method. *Physica B: Condensed Matter*. 2008;**403**:3713-3717. DOI: 10.1016/j.physb.2008.06.020
- [36] Julkapli NM, Bagheri S. Graphene supported heterogeneous catalysts: An overview. *International Journal of Hydrogen Energy*. 2014;**40**:948-979. DOI: 10.1016/j.ijhydene.2014.10.129
- [37] Yu F, Wang R. Deep oxidative desulfurization of dibenzothiophene in simulated oil and real diesel using heteropolyanion-substituted hydrotalcite-like compounds as catalysts. *Molecules*. 2013;**18**: 13691-13704. DOI: 10.3390/ molecules181113691
- [38] Phromyothin D, Phatban P, Jessadaluk S, Khemasiri N, Kowong R, Vuttivong S, et al. Growth of ZnO nanorods via low temperature hydrothermal method and their application for hydrogen production. *Materials Today: Proceedings*. 2017;**4**: 6326-6330. DOI: 10.1016/j. matpr.2017.06.134
- [39] Romero M, Henríquez R, Dalchiele EA. Electrochemical deposition of ZnO nanorod arrays onto a ZnO seed layer: Nucleation and growth mechanism. *International Journal of Electrochemical Science*. 2016;**11**:8588-8598. DOI: 10.20964/2016.10.61
- [40] Chang M, Cao X, Zeng H. Electrodeposition growth of vertical ZnO nanorod/polyaniline heterostructured films and their optical properties. *Journal of Physical Chemistry C*. 2009;**113**:15544-15547. DOI: 10.1021/jp903881d
- [41] Vigderman L, Khanal BP, Zubarev ER. Functional gold nanorods: Synthesis, self-assembly, and sensing applications. *Advanced Materials*. 2012; **24**:4811-4841. DOI: 10.1002/ adma.201201690
- [42] Chen H, Shao L, Li Q, Wang J. Gold nanorods and their plasmonic properties. *Chemical Society Reviews*. 2013;**42**:2679-2724. DOI: 10.1039/ c2cs35367a

- [43] Tian Y, Liu H, Zhao G, Tatsuma T. Shape-controlled electrodeposition of gold nanostructures. *The Journal of Physical Chemistry. B.* 2006;**110**: 23478-23481. DOI: 10.1021/jp065292q
- [44] Grzelczak M, Pérez-Juste J, Mulvaney P, Liz-Marzán LM. Shape control in gold nanoparticle synthesis. *Chemical Society Reviews.* 2008;**37**:1783-1791. DOI: 10.1039/b711490g
- [45] Ye X, Jin L, Caglayan H, Chen J, Xing G, Zheng C, et al. Improved Size-Tunable Synthesis of Monodisperse Gold Nanorods through the Use of Aromatic Additives. *ACS nano*; 2012;**6** (3):2804-2817
- [46] Koh AL, McComb DW, Maier SA, Low HY, Yang JKW. Sub-10 nm patterning of gold nanostructures on silicon-nitride membranes for plasmon mapping with electron energy-loss spectroscopy. *Journal of Vacuum Science & Technology B: Microelectronics and Nanometer Structures Processing, Measurement, and Phenomena.* 2010;**28**: C6O45-C6O49. DOI: 10.1116/1.3501351
- [47] Geng Y, Dalhaimer P, Cai S, Tsai R, Tewari M, Minko T, et al. Shape effects of filaments versus spherical particles in flow and drug delivery. *Nature Nanotechnology.* 2007;**2**:249-255. DOI: 10.1038/nnano.2007.70
- [48] Ramzannezhad A, Gill P, Bahari A. Fabrication of magnetic nanorods and their applications in medicine. *BioNanoMaterials.* 2017;**18**:1-31. DOI: 10.1515/bnm-2017-0008
- [49] Lu AH, Salabas EL, Schüth F. Magnetic nanoparticles: Synthesis, protection, functionalization, and application. *Angewandte Chemie International Edition.* 2007;**46**: 1222-1244. DOI: 10.1002/anie.200602866
- [50] Laurent S, Forge D, Port M, Roch A, Robic C, Vander Elst L, et al. Magnetic iron oxide nanoparticles: Synthesis, stabilization, vectorization, physicochemical characterizations, and biological applications. *Chemical Reviews.* 2008;**108**:2064-2110. DOI: 10.1021/cr068445e
- [51] Han C, Ma J, Wu H, Wei Y, Hu K. A low-cost and high-yield production of magnetite nanorods with high saturation magnetization. *Journal of the Chilean Chemical Society.* 2015;**60**: 2799-2802. DOI: 10.4067/S0717-97072015000100005
- [52] Khalil MI. Co-precipitation in aqueous solution synthesis of magnetite nanoparticles using iron(III) salts as precursors. *Arabian Journal of Chemistry.* 2015;**8**:279-284. DOI: 10.1016/j.arabjc.2015.02.008
- [53] Nikitin A, Khramtsov M, Garanina A, Mogilnikov P, Sviridenkova N, Shchetin I, et al. Synthesis of iron oxide nanorods for enhanced magnetic hyperthermia. *Journal of Magnetism and Magnetic Materials.* 2019;**469**: 443-449. DOI: 10.1016/j.jmmm.2018.09.014
- [54] Chen S, Feng J, Guo X, Hong J, Ding W. One-step wet chemistry for preparation of magnetite nanorods. *Materials Letters.* 2005;**59**:985-988. DOI: 10.1016/j.matlet.2004.11.043
- [55] Satuła D, Kalska-Szostko B, Szymański K, Dobrzyński L, Kozubowski J. Microstructure and magnetic properties of iron oxide nanoparticles prepared by wet chemical method. *Acta Physica Polonica A.* 2008;**114**:1615-1621. DOI: 10.12693/APhysPolA.114.1615
- [56] Ahmad M, Ahmad N, Aslam M. Synthesis of iron oxide nanorods. *Advanced Science Focus.* 2013;**1**: 150-155. DOI: 10.1166/asfo.2013.1014

- [57] Si JC, Xing Y, Peng ML, Zhang C, Buske N, Chen C, et al. Solvothermal synthesis of tunable iron oxide nanorods and their transfer from organic phase to water phase. *CrystEngComm*. 2014;**16**: 512-516. DOI: 10.1039/c3ce41544a
- [58] Sun H, Chen B, Jiao X, Jiang Z, Qin Z, Chen D. Solvothermal synthesis of tunable electroactive magnetite nanorods by controlling the side reaction. *Journal of Physical Chemistry C*. 2012;**116**:5476-5481. DOI: 10.1021/jp211986a
- [59] Kloust H, Zierold R, Merkl J-P, Schmidtke C, Feld A, Pösel E, et al. Synthesis of iron oxide nanorods using a template mediated approach. *Chemistry of Materials*. 2015;**27**:4914-4917. DOI: 10.1021/acs.chemmater.5b00513
- [60] Teja AS, Koh PY. Synthesis, properties, and applications of magnetic iron oxide nanoparticles. *Progress in Crystal Growth and Characterization of Materials*. 2009;**55**:22-45. DOI: 10.1016/j.pcrysgrow.2008.08.003
- [61] Hakuta Y, Ura H, Hayashi H, Arai K. Effects of hydrothermal synthetic conditions on the particle size of γ -AlO (OH) in sub and supercritical water using a flow reaction system. *Materials Chemistry and Physics*. 2005;**93**: 466-472. DOI: 10.1016/j.matchemphys.2005.03.047
- [62] Liang MT, Wang SH, Chang YL, Hsiang HI, Huang HJ, Tsai MH, et al. Iron oxide synthesis using a continuous hydrothermal and solvothermal system. *Ceramics International*. 2010;**36**: 1131-1135. DOI: 10.1016/j.ceramint.2009.09.044
- [63] Piao Y, Kim J, Bin Na H, Kim D, Baek JS, Ko MK, et al. Wrap-bake-peel process for nanostructural transformation from B-FeOOH nanorods to biocompatible iron oxide nanocapsules. *Nature Materials*. 2008;**7**: 242-247. DOI: 10.1038/nmat2118
- [64] He S, Guo Z, Zhang Y, Zhang S, Wang J, Gu N. Biosynthesis of gold nanoparticles using the bacteria *Rhodospseudomonas capsulata*. *Materials Letters*. 2007;**61**:3984-3987. DOI: 10.1016/j.matlet.2007.01.018
- [65] Konishi Y, Tsukiyama T, Tachimi T, Saitoh N, Nomura T, Nagamine S. Microbial deposition of gold nanoparticles by the metal-reducing bacterium *Shewanella algae*. *Electrochimica Acta*. 2007;**53**:186-192. DOI: 10.1016/j.electacta.2007.02.073
- [66] Gade A, Gaikwad S, Duran N, Rai M. Green synthesis of silver nanoparticles by *Phoma glomerata*. *Micron*. 2014;**59**:52-59. DOI: 10.1016/j.micron.2013.12.005
- [67] Mohammed Fayaz A, Balaji K, Kalaichelvan PT, Venkatesan R. Fungal based synthesis of silver nanoparticles-An effect of temperature on the size of particles. *Colloids Surfaces B Biointerfaces*. 2009;**74**: 123-126. DOI: 10.1016/j.colsurfb.2009.07.002
- [68] Rajeshkumar S, Malarkodi C, Paulkumar K, Vanaja M, Gnanajobitha G, Annadurai G. Intracellular and extracellular biosynthesis of silver nanoparticles by using marine bacteria *Vibrio Alginolyticus*. *International Journal of Nanoscience and Nanotechnology*. 2013;**3**:21-25
- [69] Wong CC, Casado IT, Álvarez YC, Legón ZM. Caracterización clínico-epidemiológica de la miopía en la población infantil de un municipio de Venezuela. *Revista Cubana de Pediatría*. 2011;**83**:149-157. DOI: 10.1007/s10853-008-2745-4
- [70] Strategies OM, Author B, Hedenstr A, Society A, Url MS, Linked UTCR. Microalga *Scenedesmus* sp.: A potential low-cost green machine for silver

nanoparticle synthesis. 2015;**90**:
1298-1309

[71] Husseiny SM, Salah TA, Anter HA. Biosynthesis of size controlled silver nanoparticles by *Fusarium oxysporum*, their antibacterial and antitumor activities. Beni-Suef Univ J Basic Appl Sci. 2015;**4**:225-231. DOI: 10.1016/j.bjbas.2015.07.004

[72] Mishra A, Tripathy SK, Wahab R, Jeong SH, Hwang I, Yang YB, et al. Microbial synthesis of gold nanoparticles using the fungus *Penicillium brevicompactum* and their cytotoxic effects against mouse mayo blast cancer C2C12cells. Applied Microbiology and Biotechnology. 2011;**92**:617-630. DOI: 10.1007/s00253-011-3556-0

[73] Pimprikar PS, Joshi SS, Kumar AR, Zinjarde SS, Kulkarni SK. Influence of biomass and gold salt concentration on nanoparticle synthesis by the tropical marine yeast *Yarrowia lipolytica* NCIM 3589. Colloids Surfaces B Biointerfaces. 2009;**74**:309-316. DOI: 10.1016/j.colsurfb.2009.07.040

[74] Chauhan A, Zubair S, Tufail S, Sherwani A, Sajid M, Raman SC, et al. Fungus-mediated biological synthesis of gold nanoparticles: Potential in detection of liver cancer. International Journal of Nanomedicine. 2011;**6**: 2305-2319. DOI: 10.2147/IJN.S23195